

Mirosław Stygar
Paweł Kurtyka
Tomasz Brylewski
Waldemar Tejchman
Renata Staśko

PHYSICOCHEMICAL AND MECHANICAL PROPERTIES OF CROFER 22 APU FERRITIC STEEL APPLIED IN SOFC INTERCONNECTS

WŁAŚCIWOŚCI FIZYKOCHEMICZNE I MECHANICZNE STALI FERRYTYCZNEJ CROFER 22 APU NA INTERCONNECTORY OGNIW PALIWOWYCH SOFC

Abstract

The paper presents the results of investigations of the physicochemical and mechanical properties of the Crofer 22 APU steel designed for application in metallic interconnects forming the key components of solid oxide fuel cells (SOFCs). Microstructural and hardness studies of non-metallic inclusions and the matrix were carried out. Based on compression tests of raw Crofer 22 APU and the steel after 600 hrs of cyclic oxidation in air at 800°C, the composition of non-metallic inclusions and their influence on the strength properties of the steel were determined.

Keywords: solid oxide fuel cell, metallic interconnect, mechanical properties, cyclic oxidation, microstructure

Streszczenie

W pracy przedstawiono wyniki badań właściwości fizyko-chemicznych i mechanicznych stali Crofer 22 APU dedykowanego do zastosowań na interkonektory metaliczne będących kluczowym elementem ogniwo paliwowych SOFC. Przeprowadzono badania mikrostruktury oraz twardości wydzieleni niemetalicznych i osnowy. Na podstawie testów ściskania stali wyjściowej oraz stali poddanej cyklicznemu utlenianiu przez 600 h w powietrzu w 800°C określono skład wytrąceń niemetalicznych oraz wykazano ich wpływ na parametry wytrzymałościowe stali.

Słowa kluczowe: ogniwo paliwowe, właściwości mechaniczne, utlenianie, mikrostruktura

1. Introduction

According to both theoretical studies and application-oriented research work, solid oxide fuel cells (SOFCs) are among the most promising solutions that may in the future provide the backbone of low-emission power production. The main reason for this is the high energy efficiency which they exhibit during operation at temperatures in the range of 600–800°C. At the same time, this aspect restricts the range of materials which may be used in the construction of SOFCs to those which exhibit sufficient resistance to high-temperature corrosion as well as long-term stability in the cells' operating conditions.

The key constituent responsible for the successful operation of a fuel cell is the interconnect. At present, metallic interconnects are the most frequently applied type; not only do such interconnects collect the electrical charge built up in the PEN (Positive – cathode/ Electrolyte/Negative – anode) component and transfer it to an external receiver, but they are also a key support structure, which needs to be highly resistant to mechanical stress and wear [1, 2].

Metallic interconnect materials, which are usually based on heat-resistant ferritic steels (FSS), need to meet a number of requirements that are either technical or physico-chemical in nature, such as: low manufacturing and processing costs, a thermal expansion coefficient (CTE) similar to that exhibited by the remaining elements of the cell, high chemical stability, low permeability with respect to hydrogen and oxygen, high resistance to wear and thermal shocks and, finally, the lowest possible area-specific resistance (ASR) [3, 4]. Furthermore, the surface of these steels may be modified using the appropriate protective-conducting layers composed of ceramics, which reduces the evaporation rate of chromium and at the same time promotes the growth of a protective scale composed mainly of chromia exhibiting high electrical resistance [5–7].

Ferritic steel seems to be the material of choice for numerous reasons. Even though they operate in various gaseous media and in varying conditions – in oxidizing atmospheres on the cathode side and reducing atmosphere on the anode side of SOFCs – they maintain their dimensions very well, which prevents the generation of such stresses as these observed in the case of chromium-rich austenitic steels or super-alloys based on nickel and chromium.

This stems from the fact that ferritic steels exhibit a body-centered cubic (bcc) structure, which is complementary to the other components of the cell, as opposed to the earlier mentioned super-alloys with a face-centered cubic (fcc) structure. In addition, ferritic stainless steels are highly resistant to oxidation in aggressive gaseous atmospheres that are present in the cell (e.g. H_2 - H_2O , CH_4 - H_2O). One of the steels that have been designed and manufactured specifically with SOFC metallic interconnects in mind is the Crofer 22 APU, which is the main subject of research in the present paper [8].

2. Main goals

The main goal of research carried out on the Crofer 22 APU steel is to expand the knowledge on its physicochemical and mechanical properties, which are essential with regard to the design of SOFC interconnects. Investigations of the resistance to compression at low strain rate were of particular importance due to the specific structure and geometry of fuel cell constituents. The scheme presented in Figure 1 demonstrates the structure of a fuel cell, composed of a series of cells (Fig. 1b) arranged in stacks (Fig. 1a). A simulation of the plastic deformation of an interconnect indicates that this element of the cell is affected by compressive stress (Fig. 1c).

- Over the course of the present study, the following aspects were investigated:
- the microstructure of the raw steel, with an especially emphasized analysis of non-metallic inclusions,
 - the hardness,
 - the resistance of raw steel and steel which had undergone oxidation in cyclic conditions to compression at room temperature.

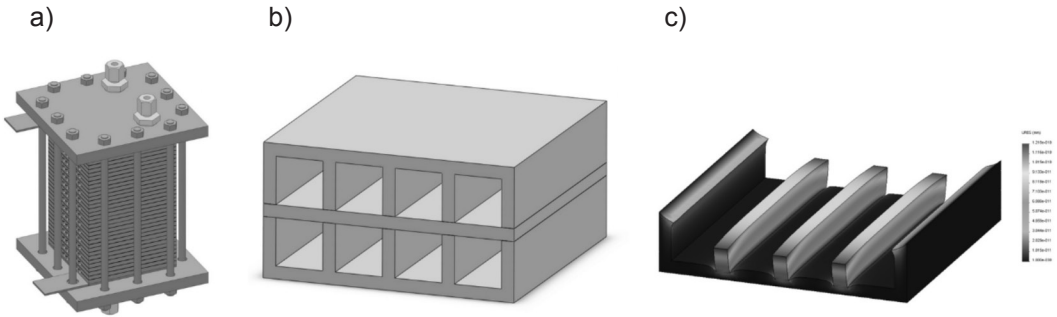


Fig. 1. Schematic representation of: a) a fuel cell stack, b) planar-type interconnect/PEN cells in a geometric system, c) compressive stress acting upon an interconnect

3. Materials and experimental methods

The material used during research was the Crofer 22 APU ferritic steel with the designations W.-No. 1.4760 X1CrTiLa22 (in the DIN EN standard) or UNS S44535 (per the ASTM standard) [9]. The steel in question was manufactured by ThyssenKrupp VDM GmbH using a license granted by Forschungszentrum Jülich, and it is dedicated for application in fuel cells, as indicated by the APU abbreviation, which stands for Auxiliary Power Unit. The steel came in the form of cast plates with a thickness of up to 20 mm. These plates underwent only basic processing during the manufacturing process, i.e. soft annealing and pickling.

The chemical composition of the investigated steel, expressed in wt.%, is presented in Table 1.

Table 1. Chemical composition of Crofer 22 APU steel (wt.%)

Element	Fe	Cr	Mn	Ti	Si	C	P	S	La
from datasheet [9]	bal.	22.0–24.0	0.30–0.80	0.03–0.20	0–0.50	0–0.03	0–0.05	0–0.02	0.04–0.20
as received	76.819	22.0	0.50	0.08	0.50	0.005	0.016	0.02	0.06

The material was ground with SiC abrasive paper with a grid of 240–2000, and polished with 9 μm and 3 μm alumina slurries. After each grinding and polishing step, the samples were rinsed in acetone using an ultrasonic cleaner.

To expose the grain boundaries of the Crofer 22 APU for the sake of tests, two formulations dedicated for stainless steels [10] were applied:

- Marble's etching reagent (50 ml HCl, 50 ml H_2O , 10 g CuSO_4),
- Lepito's etching reagent no. 1 (15 g $(\text{NH}_4)_2\text{S}_2\text{O}_8$; 250 g FeCl_3 ; 100 ml H_2O , 30 ml HNO_3).

The best results were observed for the former etchant, i.e. Marble's reagent.

The obtained polished sections were studied using an optical microscope of the Leica DM 4000 type and both light-field and dark-field techniques, and an Olympus GX51 microscope, using differential interference contrast (DIC). Morphological observations and chemical composition analyses were performed using scanning electron microscopy (SEM), JEOL 6610 LV microscope equipped with an energy dispersive X-ray spectroscopic (EDS) analyzer.

The TTX-NHT nanohardness tester supplied by CSM-Instruments was used to measure microhardness. The standard procedure utilizing the Oliver-Pharr method and the Berkovich indenter tip (pyramid angle of 142.3°) was followed. [11]. This method using usually for measuring hardness and elastic modulus by instrumented indentation techniques has widely been adopted and used in the characterization of small-scale mechanical behavior. In Oliver-Pharr method mechanical properties can be determined directly from indentation load and displacement measurements without the need to image the hardness impression. With high-resolution testing equipment, this facilitates the measurement of properties at the micrometer and nanometer scales.

The samples' resistance to compression was determined by means of a modified Instron TT-DM universal testing machine with an electronic measurement chain for measuring load and shortening/elongation of the sample. Compression tests were carried out for samples with a diameter of 3 mm and a height of 4.5 mm, with initial strain rate of ca. 10^{-5}s^{-1} . To protect the samples from the adverse effects of friction between the face of the sample and the anvil, the faces of samples were notched, and then lubricated with a graphite lubricant. The lubricant was also deposited on the anvils.

Cyclic oxidation was carried out at a temperature of 800°C in an air atmosphere; it comprised 25 cycles in total (1 cycle: 24 hrs of heating + 3 hrs of cooling) in a PESS tubular furnace with an automatic mobile roller and a DG04A recorder designer to control the operations of the furnace and to collect data.

4. Results

4.1. Microstructure and chemical composition of raw Crofer 22 APU steel

Surface investigations using metallographic optical microscopy

Figure 2 presents the microphotographs of the surface of the raw Crofer 22 APU steel, obtained using the Olympus GX51 metallographic optical microscope (Fig. 2a), and of etched raw steel, which had been investigated by means of the Leica DM 4000 (Fig. 2b) optical microscope. Observations of the non-etched raw steel revealed the presence of some inclusions with a peculiar yellowish-orange or yellowish-gray hue. The size of these inclusions ranged from 12 to $15\ \mu\text{m}$. They are objects specific to the interstitial phase, a consequence of the relation of the radii of interstitial atoms to the radii of atoms of transition metals.

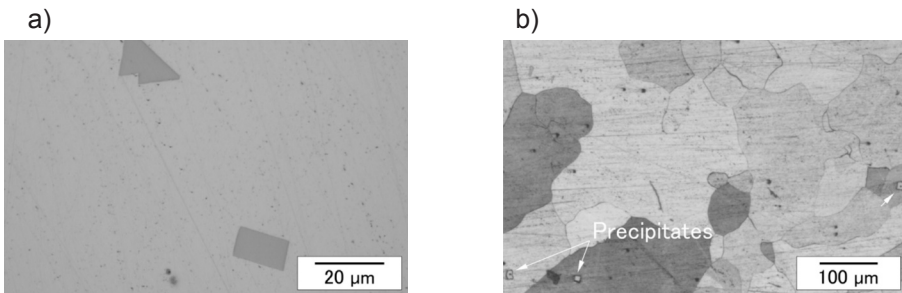


Fig. 2. Microphotographs of the raw Crofer 22 APU steel (a); raw steel etched with Marble's reagent (b)

The application of an etchant in the form of Marble's reagent made it possible to expose the grain boundaries in the raw Crofer 22 APU steel (Fig. 2b). Due to the fact that the steel had been cast in the form of a thin plate, the structure of the cast featured a uniform distribution of grains; at the same time, no cylindrical structure was observed.

SEM investigations of the steel's surface

Figure 3 shows a SEM microphotograph of the surface of the raw Crofer 22 APU steel (Fig. 3a) and the results of chemical analyses, presented in the form of X-ray distribution maps of Ti, Fe, Cr, Mn, N and C (Fig. 3b) and EDS point analyses spectra (Fig. 3c) recorded for the matrix and inclusion areas. The study of chemical composition revealed the uniform distribution of Fe, Cr and Mn in the matrix, and Ti, N and C in the inclusions. Based on the analysis of the inclusion area it may be concluded that they are composed of titanium nitrate (TiN) or titanium carbonitride (Ti(C,N)) containing a carbon-rich phase. The absence of some elements may be explained by the low resolution of the EDS method. The issue of peak overlap could be solved by using wavelength-dispersive spectroscopy (WDS), which features a much superior resolution and a higher "detectability" coefficient.

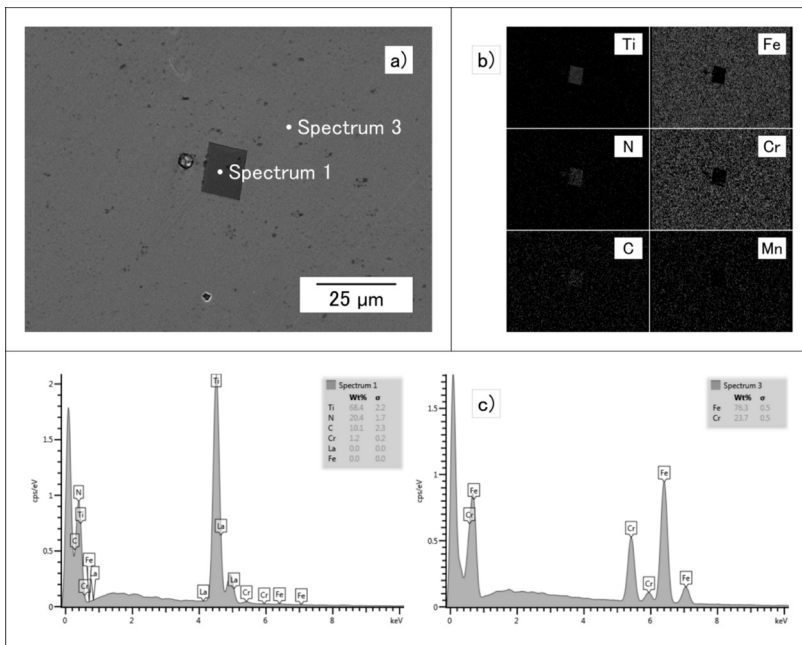


Fig. 3. Microstructure of the surface of raw Crofer 22 APU steel: a) SEM microphotographs, b) EDS element distribution map, c) EDS point analysis spectra

4.2. Hardness of raw Crofer 22 APU steel

Microhardness study and determination of strength parameters

Measurements of microhardness were carried out for at least three points, both in the matrix area and the inclusions, as demonstrated in Figure 4. These studies utilized the standard mode, i.e. by applying the load to the indenter positioned perpendicular to the surface of the sample. After the maximum intended load had been reached, the indenter was gradually withdrawn from the created indentation. The applied technique made it possible to calculate the relation between load and depth of indentation with high precision. Figures 5 and 6 illustrate this dependence.

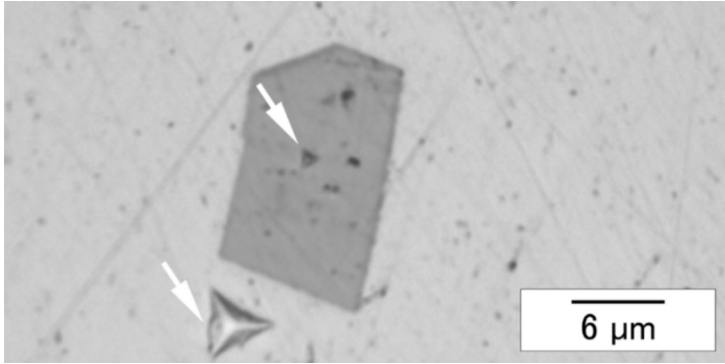


Fig. 4. Microphotograph of the surface of raw Crofer 22 APU steel with marked points of measurement in the matrix and inclusion areas

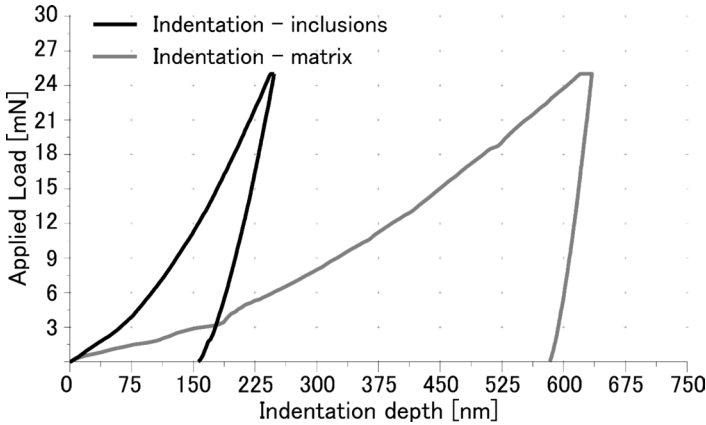


Fig. 5. Relation between applied load and indentation depth in the matrix and inclusion areas of the raw Crofer 22 APU steel, expressed vs. time

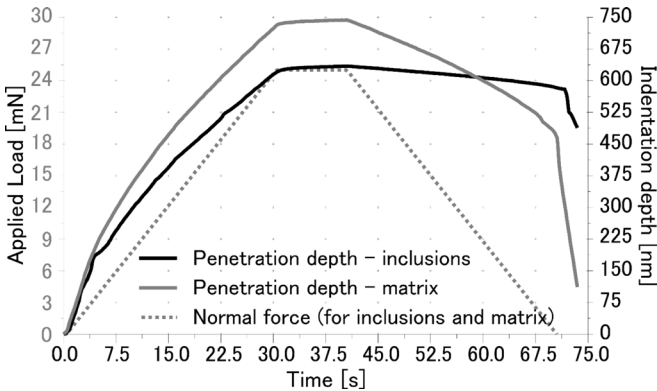


Fig. 6. Relation between applied load and indentation depth in the matrix and inclusion areas of the raw Crofer 22 APU steel

Determination of strength parameters based on hardness studies

The Oliver-Pharr method also makes it possible to determine Young's modulus by evaluating the inclination of the tangent to the initial segment of the relief curve. Moreover, the load-relief curve (Fig. 6) provides information on a number of tensile properties, which are collected in Table 2. Hardness studies were conducted in compliance with the ISO 14577 standard.

Table 2. Parameters investigated during microhardness studies and their values

Measurement parameters		
Indenter setup		Value
Measurement resolution [nm]		0.04
F_{max} (Maximum load) [mN]		25
Load factor [mN/min]		50
Relief factor [mN/min]		50
Results		
Parameter	Matrix	Inclusions
H_{IT} 0.025/30/10/30 (Hardness evaluated from F_{max}/A_p) [MPa]	3082.9	25937
E_{IT} 0.025/30/10/30 (Indentation index) [GPa]	211.87	441.79
E^* 0.025/30/10/30 (Reduced Young modulus) [GPa]	232.82	485.48
CIT 0.025/30/10 (Creep coefficient during indentation) [%]	2.48	1.85
R_U 0.025/30/10 (Indentation relaxation) [%]	0.10	0.11
ν (Poisson number)	0.30	0.30

Analysis of microhardness of inclusions in the steel

Based on a detailed analysis of the microhardness of the raw Crofer 22 APU steel, a remarkable consistency between the calculated Young modulus and the literature data [12, 13] was observed. However, after converting the obtained data to Vickers hardness (HV), it became apparent that the measurement performed by means of the TTX-NHT nano-hardness tester yielded a different hardness than the value given in the specifications of the steel [12]. Disregarding the lower hardness of the inclusions, which are not sufficiently numerous so as to make a difference, there is a significant discrepancy between the observed values and those stated by the manufacturer.

The measurement of hardness in the area of inclusions on the surface of the raw Crofer 22 APU steel yielded important insight on the type of non-metallic compound, and confirmed the observations made during EDS spectroscopic studies. The results discussed in this section are presented in Table 3.

Table 3. Comparison of Young modulus and hardness values with data found in literature

Hardness of matrix and Young modulus			
Parameter	Mean value (10 measurements)	Literature data [10]	Literature data [12]
Young modulus [GPa]	232.82	220	214
Hardness of matrix [HV]	285.51	70 – 90 [HRB] = 125 – 185 [HV] (for materials with thickness ≥ 0.38 mm)	–
Hardness of inclusion			
Parameter	Mean value (10 measurements)	Literature data [13]	Literature data [14–16]
Hardness of inclusion [HV]	2402	–	–
Hardness of TiN	–	2000	2400 – 2600
Hardness of TiC	–	1300	–
Hardness of Ti(C,N)	–	–	4400 – 4600

4.3. Mechanical properties of raw Crofer 22 APU steel and the steel after cyclic oxidation

Investigation of mechanical properties via compression tests of raw steel

The static compression test is one of the basic tests – aside from the static tension test – used to determine the mechanical properties of materials. The objective of the conducted compression test was to evaluate the stress – strain relation, which might be used to determine the following parameters: the values of stresses that result in the destruction of the material, the values of mechanical properties such as: the yield strength or yield point of a material and the deformation energy of the sample.

In addition, in order to verify expectations regarding the isotropy of mechanical properties, samples were cut from the raw material along axes x, y and z (corresponding to the plates' geometry, i.e. y axis – height, x and z axis – length and width), as illustrated by the scheme in Figure 7. The cylinders produced in this way underwent compression tests. The obtained curves are presented in Figure 8, and they are almost identical, and confirm the material's isotropy.

Once isotropy had been confirmed, it was not necessary to perform a separate series of tests for samples cut along each of the plates' axes.

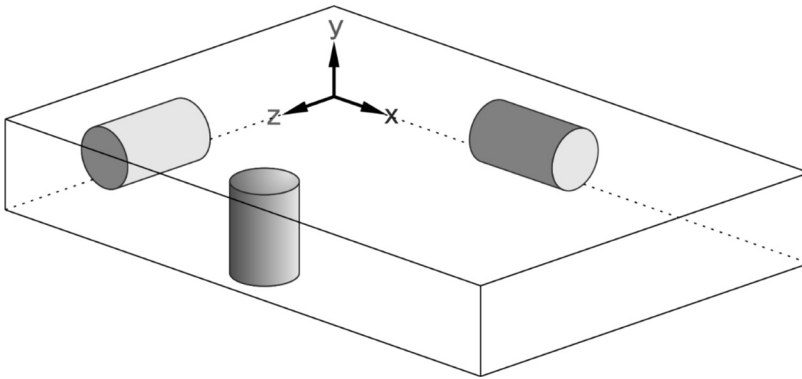


Fig. 7. A scheme illustrating the extraction of Crofer 22 APU samples for isotropic tests

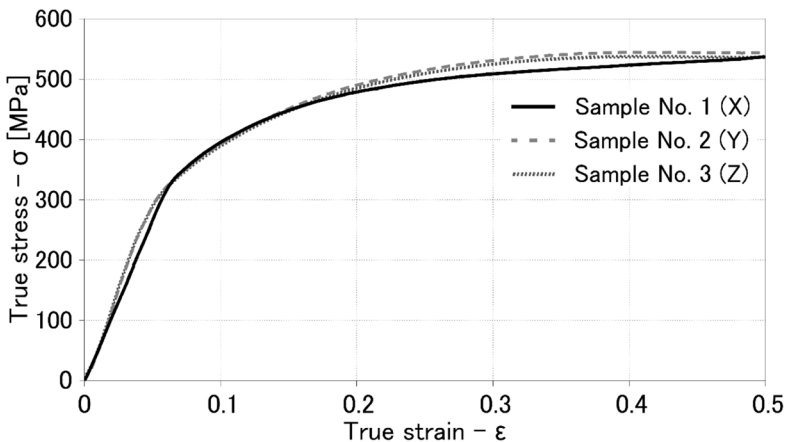


Fig. 8. Mechanical characteristics of raw Crofer 22 APU samples cut along each axis during compression tests

Studies of mechanical properties of steel after cyclic oxidation during compression tests

Figure 9 shows the behavior of the raw Crofer 22 APU steel as well as that of steel which had undergone oxidation under cyclic temperature conditions, i.e. conditions which reflect the typical, non-continuous operation of a fuel cell in an air atmosphere at 800°C; 25 cycles of 24 hrs each were initiated, for a total of 600 hrs. The obtained results revealed an increased mechanical resistance of the Crofer 22 APU steel oxidized in cyclic conditions in comparison to the raw steel, under maximum load. It may be presumed that this effect is a consequence of an effective reinforcement of the matrix not only by inclusions based on TiN or Ti(C,N), but also by numerous precipitates of silicon and titanium oxides located near the surface layer of the steel. These oxides were formed as a result of internal oxidation of silicon and titanium during long-term oxidation of the studied ferritic steel [17]. However, the proper investigation of this effect would require significantly longer cyclic oxidation, i.e. up to 1500 h.

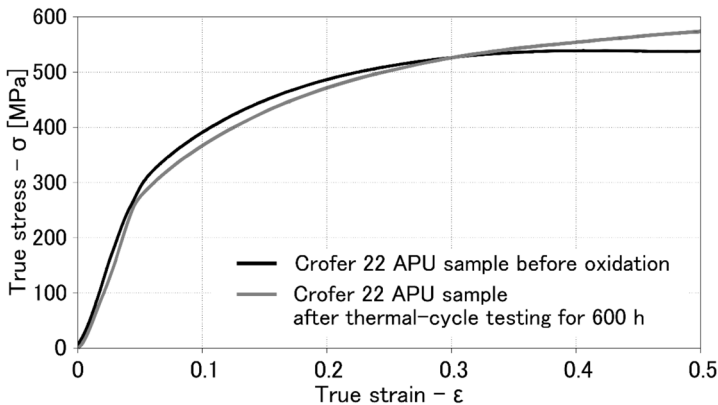


Fig. 9. Behavior of raw Crofer 22 APU samples and steel after 25 cycles of oxidation in air at 800°C, as observed during compression tests

5. Discussion and conclusions

Significant insight was gained during the investigation of the properties of non-metallic inclusions formed in the Crofer 22 APU. It is well-known that adding alloying elements such as Ti or Nb to ferritic steels results in the removal of C and N, which leads to improved corrosion resistance [18]. The titanium found in the Crofer 22 APU steel binds with nitrogen and carbon. However, it appears that the size of these inclusions exceeds the values that have so far been reported in the literature [19, 20].

According to the literature data, the size of the inclusions ranges from 4 to 10 μm . Over the course of the present study, inclusions even twice this size have been identified; this is likely not directly related to the nominal compositions of the steels, which feature similar content of alloying additions. To explain this phenomenon, it would be necessary to analyze the influence of titanium inclusions on scale growth. It should be noted that carbon and nitrogen may significantly affect the steel's resistance to stress and fracturing [21]; this may be of importance during the planned resilience tests.

The conducted investigations of the microhardness of the Crofer 22 APU steel analyzed in the context of the results of chemical composition studies carried out by means of EDS lead to the conclusion that the observed non-metallic inclusions are titanium nitrates (TiN) containing a phase that is rich in carbon, forming complex titanium carbonitrates.

The obtained results of tests of mechanical strength of the Crofer 22 APU provide a significant contribution to the current knowledge on the tensile [22] and creep [9, 22] properties in various temperature ranges. Continuing this research under conditions stated in the literature should make it possible to fully evaluate the mechanical strength of the Crofer 22 APU steel and the related properties.

Research carried out under cyclic oxidation conditions is immensely significant, since stress occurs in solid oxide fuel cells as a result of mismatched thermal expansion coefficients of its components. During operation in cyclic oxidation conditions (heating and cooling) these differences further generate stresses which may lead to the spallation of the scale or the protective-conducting layers, and to the fracturing of the working elements of the cell. In this regard, the initial results of compression tests of the Crofer 22 APU steel, which indicate an increase in the resistance of the steel's matrix, are very promising.

Another phenomenon that is particularly worth explaining is the creeping of the steel in gaseous media under pressure and at a high temperature. Further studies that are to investigate this phenomenon in conditions that realistically reflect those in which fuel cells operate are scheduled for the near future.

As far as mechanical properties under cyclic oxidation conditions are concerned, it is necessary to expand the scope of the research in order to obtain a better understanding of the metallic interconnect's operation as part of a fuel cell. The planned studies will investigate steel undergoing cyclic oxidation in gaseous media (air, H_2 - H_2O mixture) operating in the cathode and anode sides of SOFCs, and in conditions of limited circulation of gases, which correspond to the flow conditions in other geometric systems, e.g. a MOLB-type fuel cell.

Acknowledgments

The study was financed from the Małopolski Fundusz Stypendialny dla doktorantów (M. Stygar). The authors would like to express their gratitude to the LabSoft staff for making the Leica DM 4000 optical microscope and the TTX-NHT nanohardness tester available for the presented investigations, and for their

References

- [1] Weber A., Ivers-Tiffée E.: Materials and concepts for solid oxide fuel cells (SOFCs) in stationary and mobile applications. *Journal of Power Sources*, 127, 2004, pp. 273–283
- [2] Zhu W.Z., Deevi S.C.: Development of interconnect materials for solid oxide fuel cells. *Materials Science and Engineering: A*, 348, 2003, pp. 227–243
- [3] Kurokawa H., Kawamura K., Maruyama T.: Oxidation behavior of Fe–16Cr alloy interconnect for SOFC under hydrogen potential gradient. *Solid State Ionics*, 168, 2004, pp. 13–21
- [4] Brylewski T.: Metaliczny interkonektor jako istotny element ogniwa paliwowego ze stałym elektrolitem tlenkowym SOFC. *Ceramic Materials*, 62, 3(2010), pp. 415–427
- [5] Zhu J.H., Zhang Y., Basu A., Lu Z.G., Paranthaman M., Lee D.F., Payzant E.A.: LaCrO₃-based coatings on ferritic stainless steel for solid oxide fuel cell interconnect applications. *Surface and Coatings Technology*, 177–178, 2004, pp. 65–72
- [6] Cabouro G., Caboche G., Chevalier S., Piccardo P.: Opportunity of metallic interconnects for ITSOFC: Reactivity and electrical property. *Journal of Power Sources*, 156, 2006, pp. 39–44
- [7] Miszczyk M., Dziekan E., Przybylski K., Brylewski T., Gaweł R.A., Kruk A.: Physicochemical properties of the materials in the system Crofer 22 APU La_{0,6}Sr_{0,4}Co_{0,2}Fe_{0,8}O₃ on interconnectors for use in SOFC. *Ceramic materials*, 64, 1(2012), pp. 131–141 (in Polish)
- [8] Fergus J.W., Zhang J., Li X., Wilkinson D.P., Hui R.: *Solid Oxide Fuel Cells Materials Properties and Performance*. CRC Press, 2008
- [9] Crofer 22 APU – Material Data Sheet No. 4046. ThyssenKrupp VDM, 2010
- [10] Vander Voort G.F.: *ASM Handbook: Volume 9: Metallography And Microstructures*. ASM International, 2004

- [11] Oliver W.C., Pharr G.M.: An improved technique for Determining Hardness elastic modulus end using load and displacement sensing indentation experiments. *Journal of Materials Research*, 7(6), (1992), pp. 1564–1583
- [12] Chiu Y-T., Lin Ch-K., Wu J-Ch.: High-temperature tensile and creep properties of a ferritic stainless steel for interconnect in solid oxide fuel cell. *Journal of Power Sources*, 196, 2011, pp. 2005–2012
- [13] Liśkiewicz T.: Hard coatings durability under fretting wear – autoreferat
- [14] Pierson H.O.: Handbook of refractory carbides and nitrides: properties, characteristics, processing, and applications. Elsevier Science, 1996
- [15] Stone D.S., Yoder K.B., Sproul W.D.: Hardness and elastic modulus of TiN based on continuous indentation technique and new correlation. *Journal of Vacuum Science and Technology A*, 9(4), 1991, pp. 2543–2547
- [16] www: Surface Solution Inc
- [17] Żurek Z., Brylewski T., Jaroń A., Chmura E.: Area specific resistance of the scale formed on Crofer 22APU ferritic steel in atmospheres containing SO₂. *Solid State Ionics*, 234, 2013, pp. 33–39
- [18] Yan H., Bib H., Lib X., Xua Z.: Microstructure and texture of Nb+Ti stabilized ferritic stainless steel. *Materials Characterization*, 59, 2008, pp. 1741–1746
- [19] Yan H., Bi H., Lib X., Xua Z.: Precipitation and mechanical properties of Nb-modified ferritic stainless steel during isothermal aging. *Materials Characterization*, 60, 2009, pp. 204–209
- [20] Abreu H.F.G., Bruno A.D.S., Tavares S.S.M., Santos R.P., Carvalho S.S.: Effect of high temperature annealing on texture and microstructure on an AISI-444 ferritic stainless steel. *Materials Characterization*, 57, 2006, pp. 342–347
- [21] Lula R.A.: Toughness of Ferritic Stainless Steels: A Symposium. ASTM International, 1980
- [22] Chiu Y-T., Lin Ch-K., Wu J-Ch.: High-temperature tensile and creep properties of a ferritic stainless steel for interconnect in solid oxide fuel cell. *Journal of Power Sources*, 196, 2011, pp. 2005–2012